Available online at www.sciencedirect.com

SCIENCE DIRECT

Brain Research 1024 (2004) 59–76

BRAIN RESEARCH

www.elsevier.com/locate/brainres

Research report

Sensitive indicators of injury reveal hippocampal damage in C57BL/6J mice treated with kainic acid in the absence of tonic–clonic seizures

Stanley Anthony Benkovic, James Patrick O'Callaghan, Diane Bemis Miller*

Toxicology and Molecular Biology Branch, Centers for Disease Control and Prevention–National Institute for Occupational Safety and Health, 1095 Willowdale Road, Mailstop 3014, Morgantown, WV 26505, United States

Accepted 6 July 2004
Available online 1 September 2004

Abstract

Sensitive indices of neural injury were used to evaluate the time course of kainic acid (KA)-induced hippocampal damage in adult C57BL/6J mice (4 months), a strain previously reported to be resistant to kainate-induced neurotoxicity. Mice were injected systemically with saline or kainate, scored for seizure severity (Racine scale), and allowed to survive 12 h, one, three, or seven days following which they were evaluated for neuropathological changes using histological or biochemical endpoints. Most kainate-treated mice exhibited limited seizure activity (stage 1); however, cupric-silver and Fluoro-Jade B stains revealed significant damage by 12 h post-treatment. Immunohistochemistry and immunoassay of glial fibrillary acidic protein and lectin staining revealed a strong treatment-induced reactive gliosis and microglial activation. Immunostaining for immunoglobulin G revealed a kainate-induced breach in the blood–brain barrier. Nissl and hematoxylin stains provided little information regarding neuronal damage, but revealed the identity of non-resident cells which infiltrated the pyramidal layer. Our data suggest sensitive indicators of neural injury evaluated over a time course, both proximal and distal to treatment, are necessary to reveal the full extent of neuropathological changes which may be underestimated by traditional histological stains. The battery of neuropathological indices reported here reveals the C57BL/6J mouse is sensitive to excitotoxic neural damage caused by kainic acid, in the absence of tonic–clonic seizures.
Published by Elsevier B.V.

Theme: Disorders of the nervous system
Topic: Neurotoxicity

Keywords: Excitotoxicity; Neuropathology; Gliosis

1. Introduction

Kainic acid (KA) is a naturally occurring analog of the excitatory amino acid neurotransmitter glutamate, and has been used for several decades as a neurotoxic lesioning tool. Kainate intoxication has been historically evaluated in rat brain [36,37,43,58,60,71]; however, since the advent of transgenic technology, mice have become a popular animal model to investigate gene deletion/over-expression, and the need exists for re-evaluation of neurotoxic agents in wild-type and transgenic mice. Further, different strains of mice may react variably to

Abbreviations: ABC, avidin–biotin complex; ANOVA, analysis of variance; BBB, blood–brain barrier; BCA, bicinchoninic acid; CA1, cornu ammonis region 1; CA3, cornu ammonis region 3; DAB, 3–3′ diaminobenzidine tetrahydrochloride; DG, dentate gyrus; DPBS, Dulbecco's modified phosphate-buffered saline; ELISA, enzyme-linked immunosorbent assay; FJB, Fluoro-Jade B; GFAP, glial fibrillary acidic protein; HRP, horseradish peroxidase; i.e., id est; IgG, immunoglobulin G; i.p., intraperitoneal; IsoB4, *Griffonia simplicifolia* isolectin B4; KA, kainic acid; NIOSH, National Institute for Occupational Safety and Health; NSA, NeuroScience Associates; PBS, phosphate-buffered saline; PMDG, polymorphic layer of the dentate gyrus; RT, room temperature; SDS, sodium dodecyl sulfate; S.E.M., standard error of the mean

* Corresponding author. Tel.: +1 304 285 5732; fax: +1 304 285 5708.
E-mail address: dum6@cdc.gov (D.B. Miller).

0006-8993/$ - see front matter. Published by Elsevier B.V.
doi:10.1016/j.brainres.2004.07.021

chemical agents requiring evaluation of both inbred and outbred strains. This series of experiments was designed to evaluate the effects of the excitotoxicant kainic acid in the most commonly used inbred strain across scientific disciplines: C57BL/6.

Our laboratory is investigating the ability of stress to alter the susceptibility of the brain to known neurotoxic agents [19,31–33]. Recently, we have begun to examine the impact of stress on the neurotoxicity of agents targeting the hippocampus, a brain area reported to be compromised by both stress and a variety of toxic insults [5,20,28,36,51–53,58,60,71]. One particular focus has been to determine whether stress will alter innate "susceptibility" to hippocampal neurotoxicants. Recent literature reports suggest frequently used mouse strains displayed pronounced differences in the hippocampal response to systemic kainic acid administration [55]. Responses to both stress and neurotoxicity are a consequence of underlying genetic factors; therefore, we sought to utilize several inbred strains with documented genetic differences in order to investigate "susceptibility" across strains. The purpose of this series of experiments was to evaluate the basic effects of kainic acid intoxication in adult C57BL/6J mice, and develop a model with which to subsequently examine the consequences of stress on treatment-induced hippocampal neurotoxicity.

In a comparison of several inbred mouse strains, systemic treatment with kainic acid produced equivalent seizure activity across strains; however, C57BL/6 mice were reported to be "resistant" to hippocampal pyramidal cell damage and loss apparent in a "susceptible" strain, FVB/N [55]. In our initial attempts to obtain evidence of this reported differential vulnerability, we examined levels of the astrocyte-localized intermediate filament protein, glial fibrillary acid protein (GFAP), and found KA induced a reactive gliosis and elevated protein levels in both strains [4]. Elevated levels of GFAP are known to accompany a wide variety of different types of neural injury in both rat and mouse [11,25,40,41,45]; consequently, we believed an extensive examination of potential neurotoxicity caused by kainic acid in C57BL/6J was warranted.

Here, we describe the results of our evaluation of kainate-induced neurotoxicity in C57BL/6J mice utilizing both traditional and specialized indicators of histopathological damage including: Nissl; hematoxylin; cupric-silver; Fluoro-Jade B (FJB); lectin; GFAP; and immunoglobulin G (IgG) stains. Histopathological sequelae as a consequence of vehicle or kainic acid injection were scored using a semi-quantitative rating scale, and differences between treatment groups were evaluated by non-parametric statistics. Levels of GFAP in experimental animals were quantified by ELISA in order to evaluate the extent and time course of toxicant-induced reactive gliosis.

2. Materials and methods

2.1. Chemicals

Reagent chemicals were purchased from Sigma-Aldrich (St. Louis, MO), and Fisher Scientific (Pittsburgh, PA).

2.2. Animals

Male C57BL/6J mice (Jackson Laboratories) were purchased at 6–8 weeks of age, group housed on a 12/12 light/dark cycle with access to food and water ad libitum, and used in experiments at an age of 4 months. All procedures were performed under protocols approved by the NIOSH Animal Care and Use Committee, and efforts were made to minimize the number of animals used and their suffering (NIOSH 3Rs policy: reduction, refinement, replacement).

2.3. Treatment and seizure scoring

To evaluate potential neurotoxicity caused by kainic acid, mice (n=45) were injected intraperitoneally (i.p.) at a dose of 35 mg/kg, before 12:00 noon, in order to minimize interactions with circadian patterns of endogenous substances such as hormones and neurotransmitters. Dosage was based on previous experimentation evaluating GFAP by ELISA in a dose–response paradigm [4]. Kainic acid (Sigma) was dissolved in 0.9% saline at 3.5 mg/ml in order to keep the injection volume below 0.5 ml. KA-induced seizures were scored for 4 h post-injection according to the Racine scale based on the following criteria: stage 1—mouth and facial movements; stage 2—head nodding; stage 3—forelimb clonus; stage 4—rearing; stage 5—rearing and falling [46]. Control animals (n=30) received a comparable i.p. injection of 0.9% saline (i.e., 30 g mouse injected with 0.3 ml saline).

2.4. Tissue collection for ELISA

Mice were killed by decapitation 1, 3, 7, or 21 days following treatment, and the brain was rapidly removed and bisected. The hippocampus was dissected free-hand from the left hemisphere on a cold plate (Model TCP-2, Sigma-Aldrich) for determination of GFAP by ELISA. Samples were weighed, immediately frozen on dry ice, and stored at −70 °C until analyzed. The right hemisphere was immersion fixed in 4% paraformaldehyde for histopathological analysis using Nissl and Fluoro-Jade B staining.

2.5. GFAP ELISA

Hippocampal samples were sonicated in 10 volumes hot 1% SDS (Sigma) and total protein was determined by the BCA method [73]. GFAP content was assayed using a

sandwich ELISA [74,75]. Microtiter plates (96-well; Fisher Scientific) were coated with a rabbit polyclonal antibody to GFAP (Dako), and non-specific binding was blocked with reconstituted non-fat dry milk. Aliquots of the homogenates were diluted in sample buffer and added to the plate. Following blocking and washing steps, a mouse monoclonal antibody was incubated with the samples to "sandwich" GFAP. The product was visualized using alkaline-phosphatase conjugated anti-mouse IgG and enzyme substrate, *P*-nitrophenylphosphate (BioRad), and quantified by spectrometry at 405 nm using a plate reader (UV Max, Molecular Devices).

2.6. Fluoro-Jade B staining

Selected sections were stained with Fluoro-Jade B which was obtained as a gift from Dr. Larry Schmued [56]. Slides were immersed in a solution of 1% sodium hydroxide in 80% ethanol for 5 min, followed by immersion in 70% ethanol for 2 min, and distilled water for 2 min. The slides were transferred to 0.06% potassium permanganate for 10 min on a shaker to suppress background staining. Following a rinse in distilled water for 2 min, the slides were transferred to the staining solution for 20 min (stock FJB solution: 10 mg dye in 100 ml distilled water; 0.0004% working solution: 4 ml stock solution in 96 ml 0.1% acetic acid). The slides were washed three times for 1 min each in distilled water, and air-dried overnight. The slides were coverslipped directly with Permount (Fisher Scientific).

Initial evaluation of ELISA and histopathological data from treated mice suggested kainic acid-induced injury; therefore, we performed subsequent histological analysis on brains from an additional set of kainate-treated mice utilizing a highly sensitive indicator of brain damage, the cupric-silver neurodegeneration stain, to determine damage sites. Due to the development of an advanced histological process, MultiBrain Technology™ [65], the tissue was processed and stained by NeuroScience Associates (NSA, Knoxville, TN). MultiBrain Technology™ allows the simultaneous sectioning of control and treated brains and maximizes uniform staining across specimens. Time-course intervals for histology were based on GFAP ELISA data which indicated an elevation in protein levels by 24 h following treatment, and initial evaluation of Fluoro-Jade B staining which revealed fluorescent neurons at time points proximal to kainate treatment. Animals (n=45) were injected intraperitoneally with saline (control group, n=5) or 35 mg/kg KA (treatment group, n=40) and scored for seizure activity as described above.

2.7. Tissue collection for histopathology

Mice were allowed to recover for 12 h, 1, 3, or 7 days, were deeply anesthetized with Sleepaway (Fort Dodge Animal Health), and perfused transcardially with 100 ml wash solution (0.8% w/v sodium chloride, 0.4% w/v dextrose, 0.8% w/v sucrose, 0.023% w/v anhydrous calcium chloride, 0.025% w/v anhydrous sodium cacodylate in deionized water) followed by 150 ml perfusion solution (4.0% w/v sucrose, 4.0% w/v paraformaldehyde, 1.072% w/v anhydrous sodium cacodylate in deionized water). Brains were allowed to harden in the skull for 7 days, were removed, stored in fixative, and delivered to NeuroScience Associates as coded samples for sectioning and staining. At NSA, 16 brains (control, n=3; KA 12 h, n=3; KA 24 h, n=4; KA 3 days, n=3; KA 7 days, n=3) were group embedded in a gelatin matrix using MultiBrain technology, frozen in isopentane, sectioned in the horizontal plane at 35 μm on an AO860 sliding microtome, and collected into 4.0% formaldehyde containing 4.2% sodium cacodylate (pH 7.2). Every sixth section was stained for Nissl [69], cupric-silver [9], or immunostained for GFAP. One serial set of unstained sections was mounted onto microscope slides for hematoxylin and Fluoro-Jade B staining at NIOSH, and one set of free-floating sections was used for lectin staining and IgG immunohistochemistry.

2.8. Nissl staining

Sections were mounted onto gelatinized (subbed) slides. They were dehydrated through alcohols prior to defatting in a chloroform/ether/alcohol solution. The slides were rehydrated and stained in 0.05% Thionine/0.08 M acetate buffer, pH 4.5. Following deionized water rinses, the slides were differentiated in 95% alcohol/acetic acid, dehydrated in a standard alcohol series, cleared in xylene, and coverslipped.

2.9. Cupric-silver neurodegeneration stain

Sections were stained with the cupric-silver neurodegeneration stain using an adaptation of the original procedure [9]. Sections cut from the MultiBrain block were collected free-floating, rinsed in PBS, and placed in an aqueous mixture of silver nitrate, copper nitrate, cadmium nitrate, pyridine, and ethanol. Sections were subsequently processed through the following sequence: acetone; silver nitrate in combination with ammonium and sodium hydroxide; and a weak formaldehyde-citric acid and ethanol solution (for reduction). Following a PBS rinse, sections were bleached in potassium ferricyanide, and incubated in sodium borate to remove unreduced silver. Following several rinses, sections were mounted on 2×3 in. glass slides, were air dried, and coverslipped.

2.10. GFAP immunohistochemistry

To visualize GFAP immunoreactivity, sections cut from the MultiBrain block were stained free-floating. Following hydrogen peroxide treatment and blocking serum, sections were immunostained with a primary polyclonal rabbit anti-

cow GFAP antibody (1:2000, Dako) for 24 h at 4°C, a goat anti-rabbit secondary antibody (1:2000, Vector Laboratories) for 30 min at RT, and an avidin–biotin–HRP complex (Vector Laboratories) for 1 h at RT. Sections were treated with diaminobenzidine tetrahydrochloride (DAB, Sigma), rinsed, mounted on gelatinized (subbed) glass slides, air dried, and coverslipped.

2.11. Hematoxylin staining

Slide-mounted sections were rehydrated in DPBS for 5 min, and incubated in Mayer's hematoxylin (Fisher Scientific) for 5 min at room temperature. Sections were rinsed for 5 min in running tap water, dehydrated for 5 min each in 75%, 95%, and 100% ethanol, cleared in xylene, and coverslipped with Permount (Fisher Scientific).

2.12. IgG staining procedure

Immunolocalization of IgG was achieved following a truncated staining protocol using a Mouse Vectastain Elite ABC kit (PK-6102, Vector Laboratories). Free-floating sections were rinsed in DPBS and transferred directly to secondary antibody solution diluted in DPBS (1:1,000 in the absence of serum) for 2 h at room temperature (RT). Following DPBS rinses, sections were incubated with tertiary ABC complex for 1 h at RT. Sections were washed, reacted with DAB (25 mg/50 ml DPBS+50 μl 30% hydrogen peroxide (Sigma)), rinsed, mounted onto 75×50 mm microscope slides, air dried, and coverslipped. Additional slides were counterstained with hematoxylin as described above, except the staining time was reduced to 2 min.

2.13. Lectin staining

Microglial cells were visualized by staining with *Griffonia simplicifolia* Isolectin B4 (IsoB4, Vector Laboratories) using a modified procedure [27]. Free-floating sections were rinsed and incubated overnight at 4 °C in biotinylated-lectin diluted to 10 μg/ml in DPBS containing divalent cations (0.1 mM calcium chloride, 0.1 mM magnesium chloride). Sections were rinsed, incubated with tertiary ABC complex for 1 h at RT, rinsed, reacted with DAB (25 mg/50 ml DPBS+50 μl 30% hydrogen peroxide), rinsed, mounted onto 75×50 mm microscope slides, air dried, and coverslipped.

2.14. Microscopy

Microscopic analysis of stained sections was performed at NIOSH on an Olympus BX-50 microscope (Olympus America) interfaced with a Spot II digital camera (Diagnostic Images) controlled by a Macintosh G4 computer (Apple Computer). Images were captured with Spot software (v3.0.5), assembled and labeled in Photoshop 6.0 (Adobe Systems), and printed on a graphics printer (NP-1600, Codonics).

2.15. Pathology scoring

Slides were scored for severity of pathological profiles following the various histological stains using a semi-quantitative 4-point rating scale. For stains which showed a presence/absence of pathology (cupric-silver, Fluoro-Jade B, Nissl, Hematoxylin, and IgG), we utilized the following scale: 0=no pathology; 1=mild pathology; 2=moderate pathology; 3=severe pathology. For stains which showed basal reactivity in control animals (GFAP and lectin), we utilized a modified scale: 1=basal staining; 2=moderate elevation; 3=high elevation. Pathology scores were determined by low magnification microscopy (4×) of four subdivisions of the hippocampus: CA1; CA3; polymorphic layer of the dentate gyrus; and granule cell layer of the dentate gyrus. Evaluation of pathology was performed by one author (SAB) and was verified by an independent observer who was blind with respect to treatment groups (BGB).

2.16. Statistical analysis

Mean GFAP levels and associated standard errors were computed using one-way ANOVA using JMP (SAS Institute). Differences between means were analyzed by the Student's *t*-test, and were considered different when probability values were less than 0.05.

Mean pathological scores and associated standard errors for hippocampal subregions of individual animals were computed using JMP (SAS Institute). Data were analyzed using a one-way non-parametric Wilcoxon/Kruskal–Wallis ANOVA, and differences in means were considered different when Prob>χ^2 values were less than 0.05.

3. Results

3.1. Seizure scoring

Mice treated with kainic acid displayed seizures which could be broadly grouped into two categories: mild and severe. Within 15 min of KA administration, all animals appeared immobile (stage 1). Over the next 30 min, approximately 35% of treated animals progressed to higher seizure states: 10% peaked at stage 2; while 25% experienced severe tonic–clonic seizures followed by death of the animal. No surviving animals peaked between stages 3 and 5. The initial biochemical (GFAP ELISA) and histological (FJB) data analyzed were from the 75% of mice treated with kainic acid which exhibited "mild" stage 1–2 seizures. On the day following kainate treatment, the mice showed no residual effects of treatment (i.e., no obvious seizure or behavioral effects). Interestingly, ani-

mals that expired from kainate treatment generally died within 24 h or at approximately 7 days post-injection. No seizure activity was observed in animals treated with saline.

3.2. GFAP ELISA

Kainic acid treatment caused a time-related elevation in total hippocampal levels of GFAP as revealed by ELISA with the maximum significant three-fold elevation at 7 days post-injection (Fig. 1). GFAP levels began increasing by 24 h following treatment, achieved significant elevation at 3 days, and resolved to control levels by 21 days.

In order to localize sites of damage, we sectioned the right hemispheres of animals in which the left hemispheres were evaluated by ELISA, and subjected them to staining with Fluoro-Jade B. In animals with a survival time proximal to treatment, we observed fluorescent neurons, indicating kainate-induced neuronal damage (data not shown). Since C57BL/6J mice were reported to be resistant to kainic acid neurotoxicity, we proposed further histopathological analysis utilizing multiple indicators of neuronal damage evaluated over a time course that coincided with the elevation of GFAP. Evaluation of the brains from animals treated with kainate revealed damage to most major brain regions; however, due to the extensive quantity of data obtained, and the specific focus of this manuscript on the hippocampal formation, extrahippocampal histopathology will be reported separately.

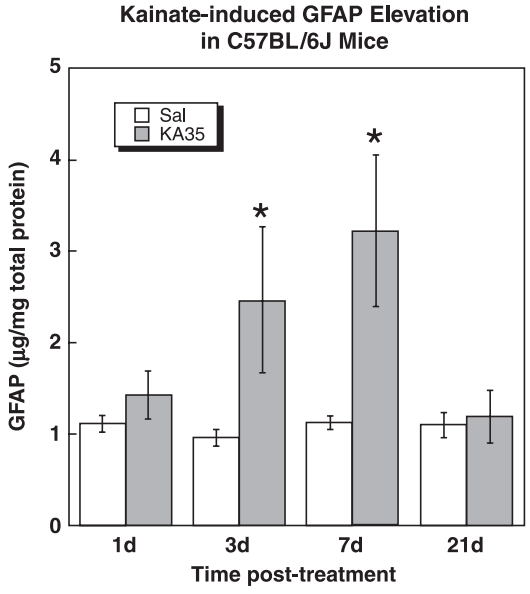

Fig. 1. Kainate treatment caused an elevation of GFAP levels by 1 day (saline n=6, 1.10±0.09; KA n=4, 1.43±0.26), which became significantly elevated by 3 days (saline n=6, 0.95±0.08; KA n=4, 2.46±0.80; p<0.046), and continued to increase through 7 days (saline n=11, 1.22±0.07; KA n=7, 3.22±0.84; p<0.008). By 21 days following treatment, GFAP levels had resolved to baseline (saline n=6, 1.10±0.14; KA n=6, 1.20±0.29).

3.3. GFAP immunohistochemistry

Evaluation of GFAP by immunohistochemistry revealed a treatment-induced reactive gliosis in hippocampus compared to control animals (Fig. 2). In saline-injected animals, basal immunostaining of GFAP was observed in all hippocampal subregions; however, immunoreactivity was noticeably less in the vicinity of CA3 (Fig. 2A). By 12 h following treatment (Fig. 2B), elevated immunostaining of GFAP was observed in all hippocampal subregions (CA1, CA3, the polymorphic layer of the dentate gyrus, and the molecular layer of the dentate gyrus) when compared to control animals. Immunoreactivity continued to increase through 24 h (Fig. 2C). By 3 days post-treatment, astrocytes appeared swollen with protein, and emanated many processes containing the intermediate filament, especially in region CA3 (Fig. 2D). By 7 days, the entire hippocampal neuropil was immunoreactive (Fig. 2E). High-magnification microscopy of GFAP immunoreactive astrocytes revealed the morphological characteristics of classical reactivity: many short, stout processes filled with the intermediate filament (Fig. 2F).

Semi-quantitative evaluation of kainate-induced GFAP immunostaining revealed morphological changes associated with activation, and a significant increase in immunoreactivity by 12 h following treatment in CA1 and CA3, which remained significantly elevated for 7 days (Fig. 3). In the polymorphic and molecular layers of the dentate gyrus, kainate treatment caused astrocyte activation and an elevation in GFAP immunoreactivity by 12 h. Levels of GFAP continued to increase and became significantly elevated compared to control animals by 24 h; protein levels remained significantly elevated through 7 days.

3.4. Cupric-silver stain

The cupric-silver neurodegeneration stain (Fig. 4) showed a time-dependent increase in argyrophilic cells relative to saline controls (Fig. 4A). Saline treated mice showed no overt cell damage, but had a small amount of silver deposition in stratum lucidum proximal to the CA1/3 transition point (see arrow in Fig. 4A). By 12 h following kainate treatment, argyrophilic cells were observed amongst pyramidal neurons in CA1 and CA3, and in the subiculum, and a few argyrophilic interneurons were observed scattered throughout stratum radiatum (Fig. 4B). By 24 h following treatment, increased numbers of argyrophilic cells were observed in CA1 and CA3, and within the polymorphic layer of the dentate gyrus (Fig. 4C). A few silver-stained neurons and fibers were observed in the parasubiculum, but the presubiculum was relatively spared. Severe argyrophilia was observed in fibers of stratum oriens, stratum radiatum, and stratum lacunosum-moleculare. The Nissl counterstain used in this preparation, neutral red, showed a zone of CA3 in which cells failed to stain (see arrow in Fig. 4C). This zone of non-staining correlated with the area of infiltration

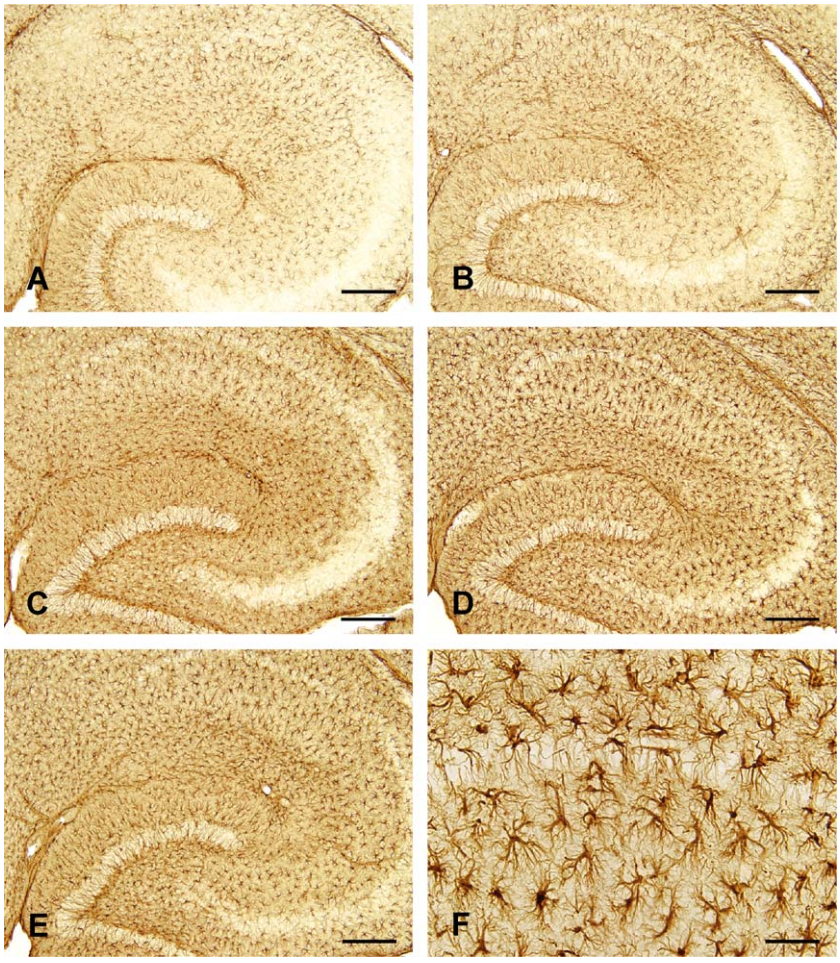

Fig. 2. GFAP immunostaining in hippocampus of mice treated with saline or KA. The hippocampus of a saline-injected animal showed basal GFAP immunostaining (A). KA enhanced immunoreactivity by 12 h following treatment (B). By 24 h, numerous immunoreactive astrocytes were observed throughout the hippocampus (C). By 3 days post-treatment, reactive astrocytes were observed in all subregions (D). At 7 days, GFAP immunoreactivity was maximal (E). High magnification of astrocytes at 7 days following treatment revealed classic activation morphology: many short, stout process filled with the intermediate filament (F). Bar in (A)–(E)=200 μm. Bar in (F)=50 μm.

of non-neuronal cells into the pyramidal layer (see below). CA1 pyramidal neurons showed deposition of silver over the extent of the cell soma. The basilar dendritic tree was highly branched and easily observed projecting into stratum oriens while the apical dendritic tree appeared less branched, but could be observed projecting through stratum radiatum and stratum lacunosum-moleculare as far as the hippocampal fissure (Fig. 4G). Argyrophilic basilar dendrites appeared twisted as they coursed through stratum oriens. Apical projections from pyramidal neurons were thicker, twisted, and had a beaded appearance along the distal length of the process. CA3 pyramidal neurons were likewise labeled, but contained more silver reaction product due to the larger size of the cell body (Fig. 4H). Basilar and apical dendritic trees could be followed into stratum oriens and stratum radiatum, respectively. In stratum oriens, argyrophilic interneurons were observed that had projections perpendicular to the axis of the pyramidal neurons, and a dense accumulation of fibers were frequently observed deep to the subarea of CA3 containing argyrophilic pyramidal neurons. Granule cells of the dentate gyrus and the corresponding mossy fibers of the stratum lucidum were relatively spared; however, occasional interneurons in the mossy fiber lamina were labeled with silver (Fig. 4I). Granule cells in the dentate gyrus were spared; however, occasional interneurons were labeled with silver. Argyrophilic mossy cells were observed within the polymorphic layer (Fig. 4J,L). These neurons had large multipolar cell bodies with several thick dendrites which could be seen to course for large distances through the polymorphic layer. In the parahippocampal gyrus, argyrophilic neurons were observed in the entorhinal cortex, and their projections into stratum moleculare were also labeled with silver. Argyrophilic fibers were also observed in stratum radiatum (Schaffer collaterals), and in the subiculum (Fig. 4K). Orientation of argyrophilic fibers appeared to be both transverse and along the septotemporal axis. By 3 days following kainate treatment, argyrophilia was attenuated in the majority of treated animals (Fig. 4D), and at 7 days post-treatment the hippocampus appeared similar to the saline

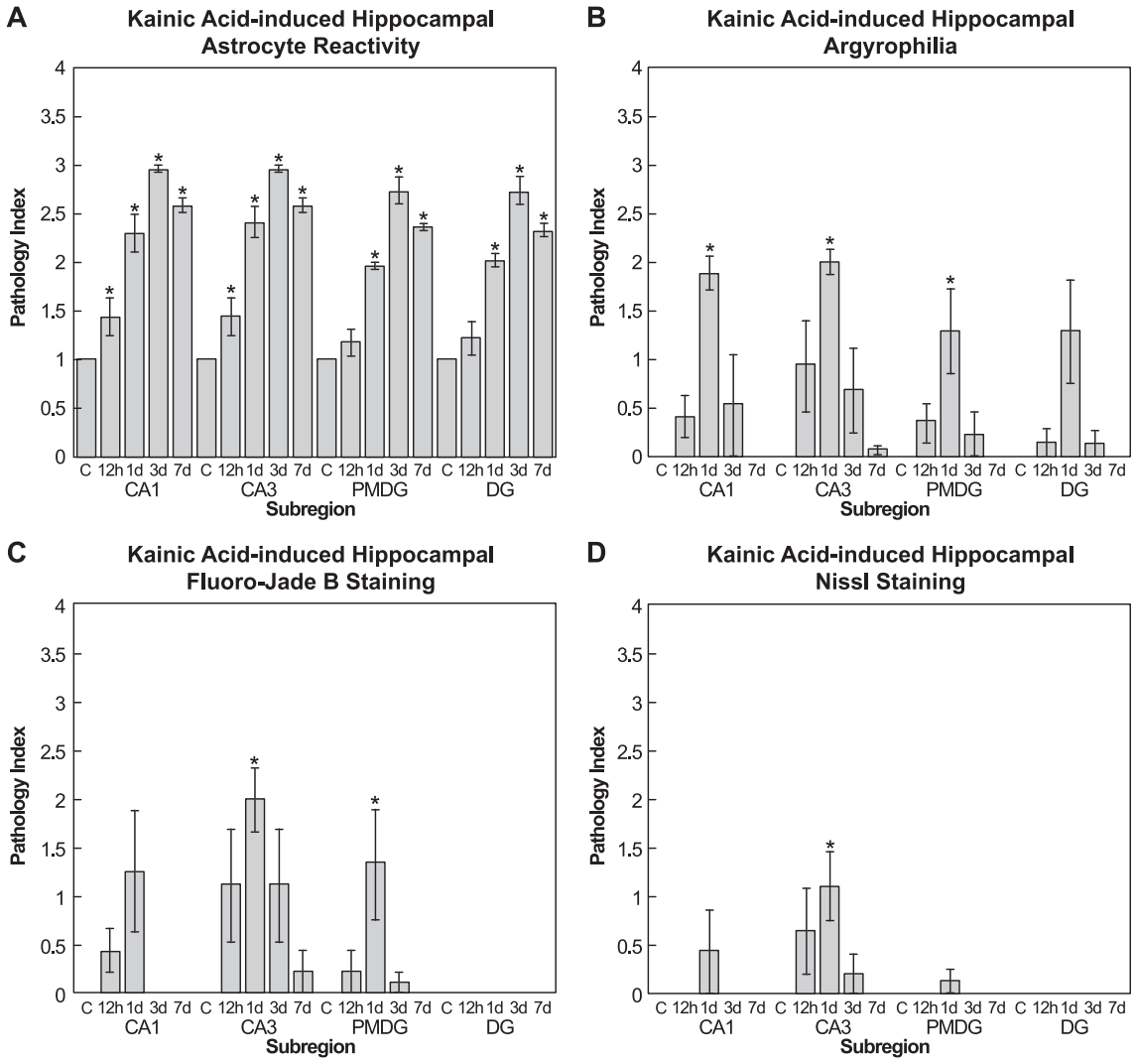

Fig. 3. Semi-quantitative analysis of histopathology in mice treated with saline or KA. (A) Kainic acid caused significant elevations in GFAP levels in CA1 and CA3 at 12 h (p=0.037 and p=0.037, respectively), 24 h (p=0.022 and p=0.026, respectively), 3 days (p=0.034 and p=0.034, respectively) and 7 days (p=0.034 and p=0.034, respectively) following treatment. In the polymorphic layer of the dentate gyrus, and the granule cell and molecular layers of the dentate gyrus (DG), GFAP levels were significantly elevated at 24 h post-treatment (p=0.022 and p=0.026, respectively), 3 days (p=0.034 and p=0.034 respectively), and 7 days (p=0.034 and p=0.037 respectively). (B) Kainic acid injection caused a significant elevation in the number of silver stained neurons and fibers in CA1, CA3, and the polymorphic layer of the dentate gyrus at 24 h post-treatment (p=0.026, p=0.028 and p=0.028, respectively). (C) Kainic acid injection caused a significantly elevated number of fluorescent neurons at 24 h following treatment in CA3 and the polymorphic layer of the dentate gyrus (p=0.022 and p=0.027, respectively). (D) Kainic acid injection caused little damage as revealed by Nissl staining. In CA3, significant pathology was observed at 24 h (p=0.028) post-treatment.

controls (Fig. 4E), except for some residual argyrophilia in stratum oriens and the subiculum of one animal. High magnification microscopic evaluation of CA3 revealed an accumulation of reduced silver in neuronal soma, axon, and dendrites, and allowed the characterization of degenerating neuronal populations and their projection patterns (Fig. 4F).

Semi-quantitative evaluation of kainate-induced argyrophilia (Fig. 3) revealed an elevation in the number of silver stained neurons and fibers by 12 h following treatment in CA1, CA3, and the polymorphic layer of the dentate gyrus. Differences between means of controls and treatment groups achieved significance by 24 h, and were attenuated to non-significant levels by 3 days post-treatment. In dentate gyrus, kainate treatment caused silver deposition onto damaged terminals of the molecular layer by 12 h; the quantity increased non-significantly by 24 h, and was attenuated by 3 days following treatment.

3.5. Fluoro-Jade B staining

The fluorochrome indicator of neuronal degeneration, Fluoro-Jade B, was used to evaluate the effects of kainate intoxication and compare the profile of damage to the cupric-silver stain (Fig. 5). Saline-injected control animals showed no staining with FJB (Fig. 5A). By 12 h following treatment, fluorescent neurons were observed in the

pyramidal layer of CA3 (Fig. 5B). At high magnification, basilar processes of stained neurons were observed projecting into stratum oriens, and apical dendrites could be seen extending into stratum radiatum. By 24 h post-treatment, fluorescent neurons were observed amongst pyramidal neurons in CA1 and CA3. FJB-labeled neurons were also observed in the polymorphic layer of the dentate gyrus, and labeled interneurons were scattered throughout stratum radiatum (Fig. 5C). By 3 days following treatment, fluorescent neurons were attenuated in quantity, and were generally observed only in CA3 (Fig. 5D). No fluorescent neurons were observed at 7 days following treatment (Fig. 5E). High-magnification microscopic evaluation of Fluoro-Jade B stained sections revealed binding of the fluorescent indicator to cell bodies and both basilar and apical processes (Fig. 5F).

Semi-quantitative evaluation of kainate-induced Fluoro-Jade B staining (Fig. 3) revealed an elevated number of fluorescent neurons by 12 h following treatment in CA1; the quantity of labeled neurons increased non-significantly by 24 h. In CA3 and the polymorphic layer of the dentate gyrus, fluorescent neurons were observed by 12 h following treatment; this quantity continued to increase and was significantly different from control animals by 24 h. No fluorescent neurons were observed in the granule cell layer of the dentate gyrus at any time-point following kainic acid treatment.

3.6. Nissl stain

Nissl staining revealed no obvious kainate-induced loss of pyramidal cells compared to saline controls (Fig. 6A);

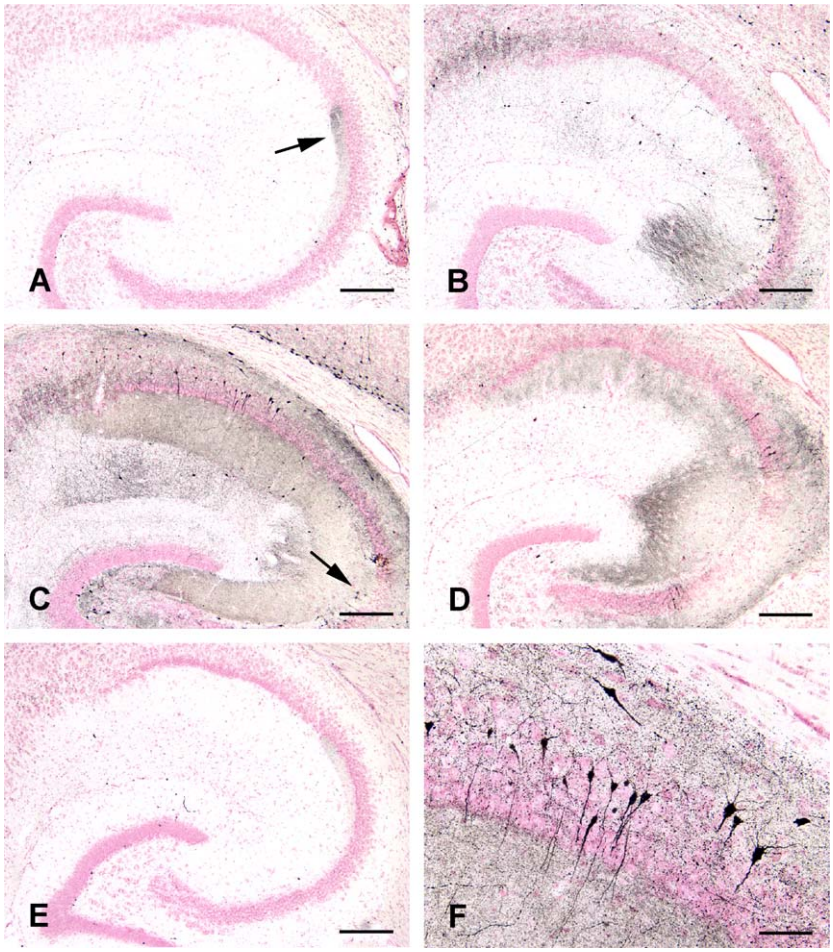

Fig. 4. Cupric-silver staining in hippocampus of C57BL/6J mice treated with saline or KA. The hippocampus of a saline-injected animal showed a small amount of silver staining in CA3 (A). By 12 h following treatment, argyrophilic cells and fibers appeared amongst pyramidal neurons in CA1 and CA3, and in the subiculum. Occasional argyrophilic interneurons were observed in stratum oriens (B), By 24 h, increased argyrophilia was observed in CA1, CA3, and the polymorphic layer of the dentate gyrus (C). At 3 days post-treatment, argyrophilia was attenuated (D), and by 7 days following treatment, the hippocampus appeared similar to the saline control (E). High magnification of CA3 at 24 h revealed silver deposition in the cell body, axon, and dendrites (F). Processes of argyrophilic CA1 pyramidal neurons can be followed through stratum radiatum to the hippocampal fissure (G). Argyrophilic CA3 pyramidal neurons and processes are observed twisting through stratum radiatum (H). Fibers terminating in stratum lucidum are relatively spared by kainate treatment; however, argyrophilic interneurons are occasionally observed (I). A band of degenerating fibers projecting from the entorhinal cortex to the inner molecular layer of the dentate gyrus is stained with silver (J). KA damaged neurons and fibers in the subiculum (K). Argyrophilic mossy cells in the polymorphic layer of the dentate gyrus (L). Bar in (A–E)=200 μm. Bar in (F)=50 μm. Bar in (G–L)=100 μm.

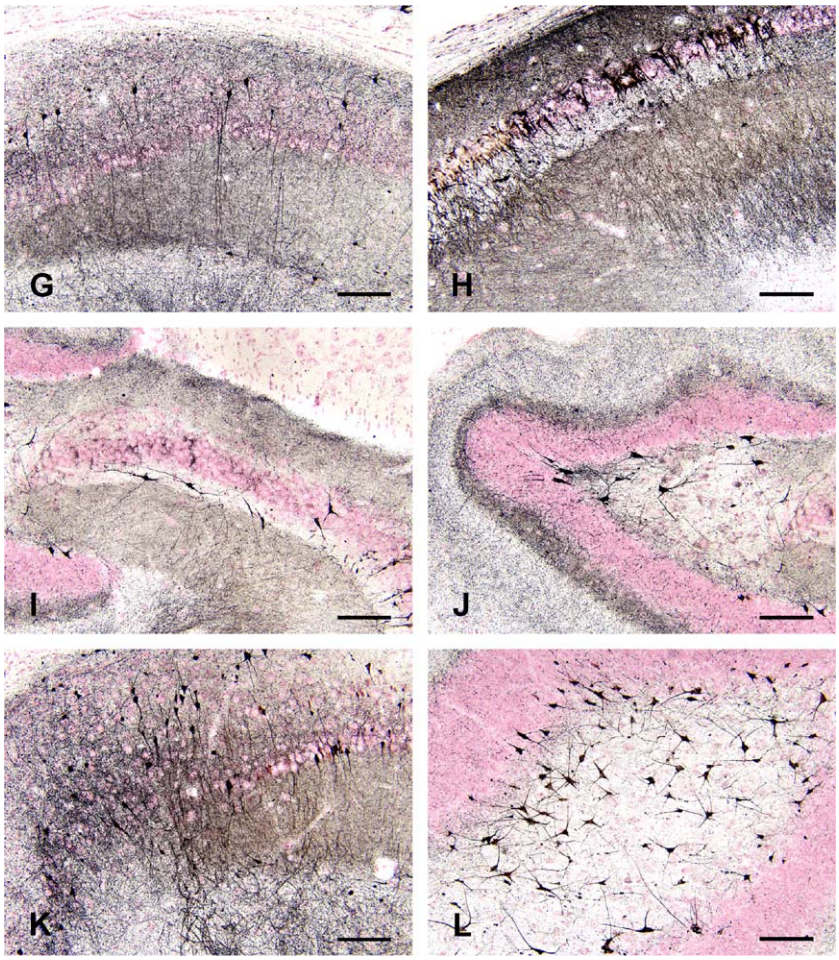

Fig. 4 (*continued*).

however, a prominent zone of non-staining was observed in CA3 at time points proximal to treatment (Fig. 6B, C, and F). Coincident with the non-staining by Nissl was the appearance of cells which morphologically resembled polymorphonuclear leukocytes (Fig. 6B, C, D, and F), i.e., small, round cells with granular cytoplasm and a multilobed nucleus. The time course of non-staining by Nissl and the infiltration of polymorphonuclear leukocytes into the pyramidal layer correlated with kainate-induced argyrophilia; however, the zone of non-staining was not argyrophilic. The infiltration was topographic, observed at septal and midlevels of the septotemporal axis, was not observed temporally, and in the majority of animals, was bilateral. At 24 h post-treatment, leukocytes were observed amongst pyramidal neurons in CA1 and within the polymorphic layer of the dentate gyrus. At 3 days post-treatment, the extent of the zone of non-staining was attenuated, and by 7 days, the hippocampus appeared indistinguishable from saline controls (Fig. 6E compare with Fig. 6A).

Semi-quantitative evaluation of Nissl staining reflected the extent of the zone of non-staining by Nissl and the influx of polymorphonuclear leukocytes into the hippocampus (Fig. 3). In CA1 and the polymorphic layer of the dentate gyrus, leukocytes were observed only at 24 h post-treatment in a few animals; however, the quantity was variable and not significantly different from controls. In CA3, an increase in the influx of leukocytes into the pyramidal layer was observed by 12 h; the quantity continued to increase and achieved significance by 24 h. By 3 days post-treatment, the extent of the zone of non-staining and the quantity of leukocytes was attenuated, and by 7 days, the hippocampus appeared similar to the saline controls.

3.7. Hematoxylin staining

To determine the identity of non-neuronal cells infiltrating the pyramidal layer, brains from animals treated with saline or KA were stained with hematoxylin (Fig. 7). No evidence of non-resident infiltration was observed in saline controls (Fig. 7A). The time course and topographic distribution of infiltrating cells was identical to that revealed by Nissl staining; however, nuclear morphology was better identified by hematoxylin staining. By 12 h following kainate treatment, the CA3 region appeared disrupted and showed infiltration of small, round cells with granular cytoplasm and a multilobed nucleus that had the histological

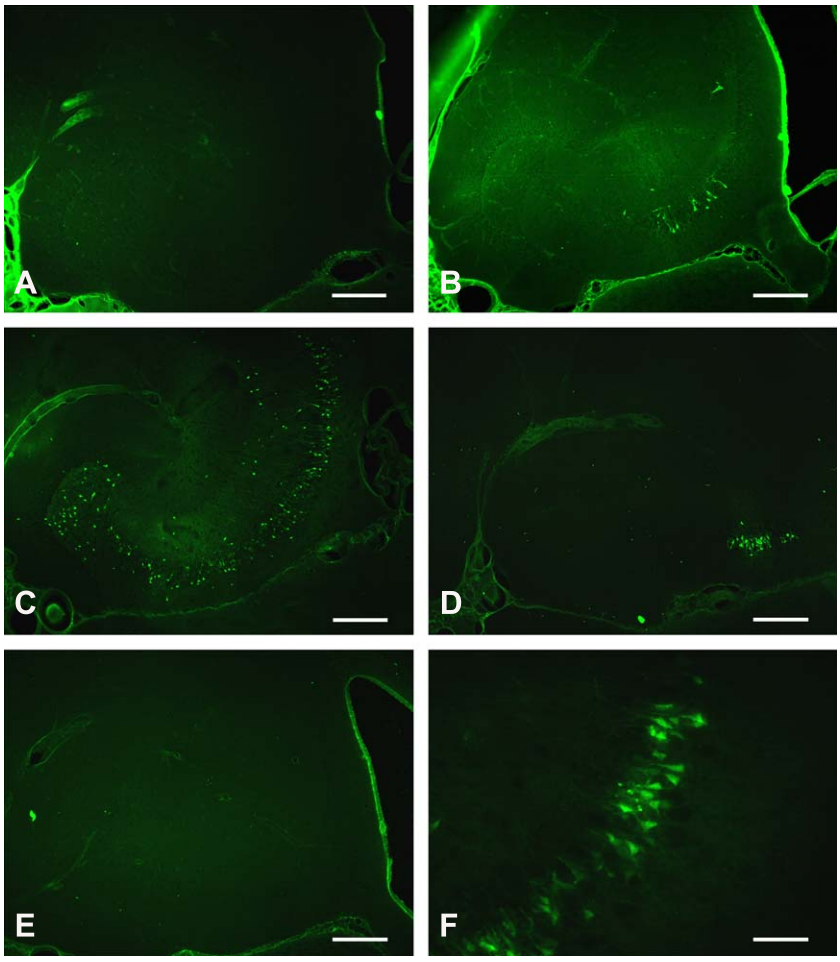

Fig. 5. Fluoro-Jade B staining in hippocampus of mice treated with saline or KA. The hippocampus of a saline-injected animal showed an absence of Fluoro-Jade B staining (A). KA caused an appearance of fluorescent neurons in the pyramidal layer by 12 h (B). By 24 h, fluorescent neurons were observed amongst pyramidal neurons, in the polymorphic layer of the dentate gyrus, and interspersed throughout the stratum radiatum (C). By 3 days following treatment, only a few fluorescent neurons were observed in subregion CA3 (D). By 7 days the hippocampus appeared similar to the saline control (E). High magnification of CA3 at 24 h following treatment showed Fluoro-Jade B binding to neuronal soma and processes (F). Bar in (A–E)=200 μm. Bar in (F)=50 μm.

characteristics of polymorphonuclear leukocytes (Fig. 7B). By 24 h post-treatment, CA3 infiltration was maximal, and many leukocytes had invaded the pyramidal layer (see arrow Fig. 7C); in a few animals, leukocytes were observed amongst pyramidal neurons in CA1 and the polymorphic layer of the dentate gyrus. By 3 days following treatment, evidence of CA3 disruption was attenuated (Fig. 7D), and by 7 days post-treatment, the hippocampus appeared similar to saline controls (Fig. 7E). High magnification microscopy revealed the morphology of the infiltrating cells, i.e., multilobed nucleus and granular cytoplasm, which was consistent with the structure of polymorphonuclear leukocytes (Fig. 7F).

Semi-quantitative evaluation of hematoxylin staining following kainate-induced damage revealed no overt neuropathology, but reflected the influx of leukocytes infiltrating the hippocampus (Fig. 8). No significant pathological profiles were observed in the granule cell layer of the dentate gyrus; however, a variable non-significant quantity of leukocytes was observed in CA1 and the polymorphic layer of the dentate gyrus only at 24 h post-treatment. In CA3, infiltrating leukocytes were observed by 12 h following kainate injection; the quantity of infiltrating cells was significantly different from saline controls by 24 h post-treatment, was attenuated by 3 days, and appeared similar to control animals by 7 days following treatment.

3.8. IgG immunostaining

In brains from animals injected with KA, IgG immunohistochemistry revealed extravasation of immunoglobulin into the hippocampus indicating a breach of the blood–brain barrier (Fig. 9). No IgG was detected in saline-injected controls (Fig. 9A). By 12 h following treatment, the hippocampal neuropil contained considerable immunoreaction product, and IgG immunostained neurons were observed in the pyramidal layer of CA3 (Fig. 9B). The topographical distribution of IgG immunoreactive cells correlated with the areas of non-staining and leukocyte infiltration by Nissl and hematoxylin stains. By 24 h, faintly

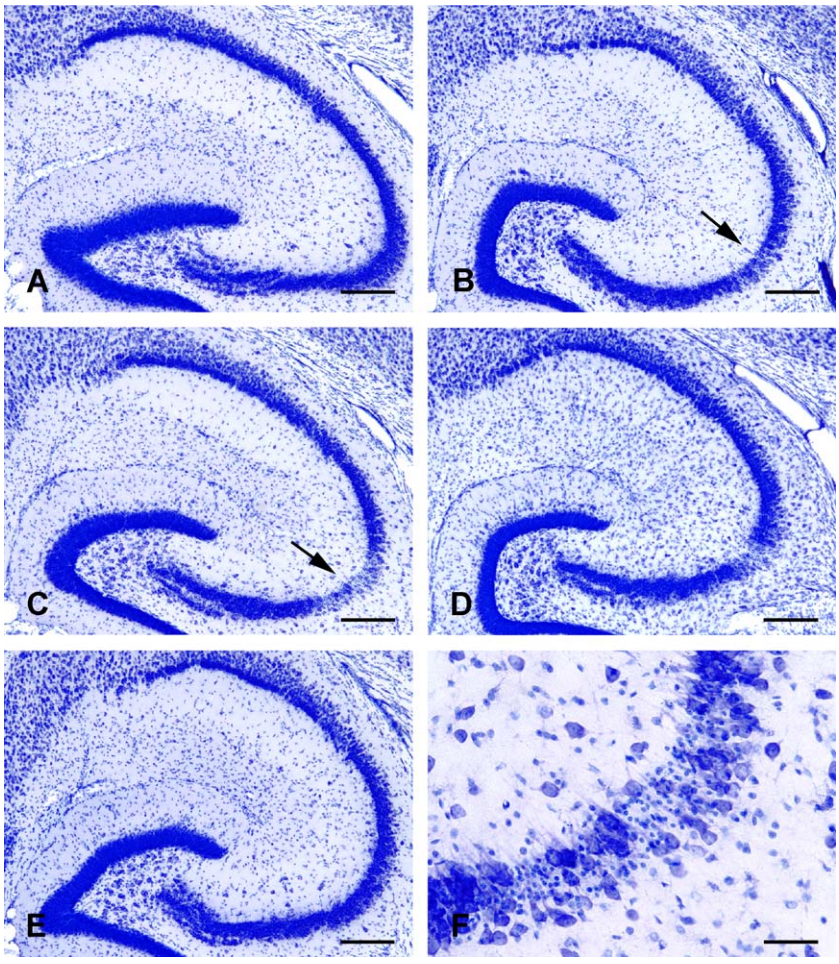

Fig. 6. Nissl staining of hippocampus in C57BL/6J mice treated with saline or KA. The hippocampus of a saline-injected animal showed control Nissl staining (A). By 12 h following KA injection, a small zone of CA3 neurons was observed which failed to stain (arrow in B). This zone was topographically localized to septal and midlevels along the septotemporal axis, and was observed to increase in size by 24 h (arrow in C). At 3 days (D) and 7 (E) days following treatment, the hippocampus appeared similar to the saline control. High magnification of CA3 at 24 h revealed the presence of non-neuronal cells infiltrating the pyramidal layer (F). Bar in (A–E)=200 μm. Bar in (F)=50 μm.

immunoreactive profiles of microglial cells were observed throughout the hippocampus (Fig. 9C). At 3 days (Fig. 9D) and 7 days (Fig. 9E) post-treatment, immunoreactivity was attenuated nearly to control levels. High magnification microscopic evaluation of IgG immunoreactive cells dispersed throughout the hippocampal neuropil at 24 h post-treatment revealed the morphology to be similar to microglia (Fig. 9F).

Semi-quantitative evaluation of IgG immunoreactivity following kainic acid intoxication revealed treatment-induced extravasation of plasma-derived immunoglobulin into the parenchyma of all hippocampal subregions with a similar profile of intensity and time course (Fig. 8). In CA1, CA3, the polymorphic layer of the dentate gyrus, and the molecular layer of the dentate gyrus, elevated levels of parenchymal IgG and immunoreactive microglial cells were observed by 12 h following injection; the quantity of immunoreactive cells and magnitude of IgG extravasation became significantly elevated compared to control animals by 24 h post-treatment. By 3 days following treatment, IgG immunoreactivity was similar to saline-injected control animals.

3.9. Lectin staining

Brains from mice treated with KA and stained with *G. simplicifolia* Isolectin B4 revealed a treatment-induced microglial response compared to saline-injected controls (Fig. 10). Virtually no reactive microglial cells were observed in saline-injected controls; however, occasional processes were lectin stained (Fig. 10A). By 12 h following kainate, many processes of lectin stained cells were observed throughout the hippocampal neuropil (Fig. 10B). By 24 h, numerous profiles of microglial cells were observed in all hippocampal regions, and lectin staining was observed in processes and the cell bodies (Fig. 10C). By 3 days post-treatment, lectin staining was attenuated; however, processes of microglial cells were persistently observed in the hippocampal strata (Fig. 10D). By 7 days following treatment, lectin staining was further attenuated,

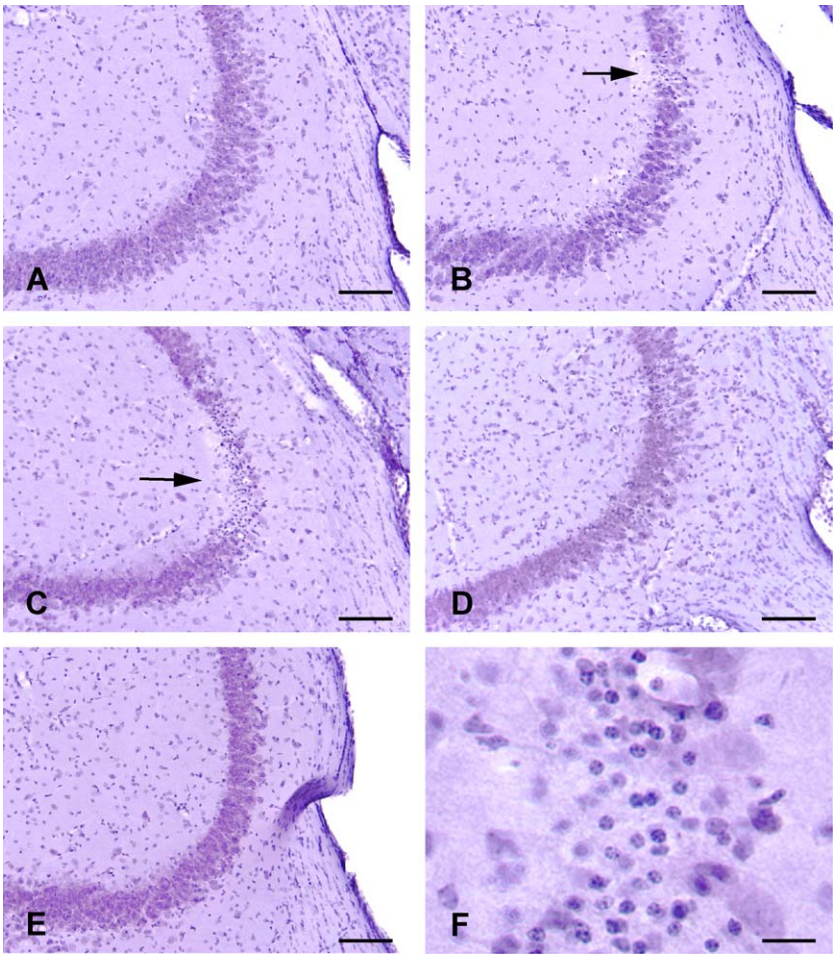

Fig. 7. Hematoxylin staining in hippocampus of mice treated with saline or KA. The hippocampus of a saline-injected animal showed control hematoxylin staining (A). By 12 h following KA treatment (arrow in B), an influx of leukocytes into the pyramidal layer was observed. By 24 h post-treatment, both the size of the region of infiltration and the number of invading leukocytes was increased (arrow in C). At 3 days, the size of the zone of infiltration and the quantity of leukocytes was attenuated (D). By 7 days following treatment, the hippocampus appeared similar to the saline control (E). High magnification of CA3 at 24 h revealed the extent of leukocytic infiltration of the pyramidal layer (F). Bar in (A–E)=100 μm. Bar in (F)=17 μm.

yet still remained elevated compared to saline-injected controls in region CA3 of a few animals (Fig. 10E). High magnification microscopic evaluation of lectin stained cells revealed the morphology to be consistent with microglia (Fig. 10F).

Semi-quantitative evaluation of microglial reactivity following kainic acid treatment revealed enhanced lectin staining and treatment-induced changes in microglial morphology compared to control animals (Fig. 8). In CA1, CA3, the polymorphic layer of the dentate gyrus, and the granule cell and molecular layers of the dentate gyrus, kainate treatment caused the appearance of activated microglial cells with a similar time course and intensity. By 12 h following treatment, processes of microglia were observed in all hippocampal regions; this quantity continued to increase compared to control animals and achieved significance by 24 h post-treatment. By 2 days following treatment, the quantity and intensity of the lectin stain was attenuated, and by 7 days, further attenuation was observed except in region CA3.

4. Discussion

We detected and quantified neuropathological changes in the hippocampus of C57BL/6J mice due to damage caused by systemic administration of kainic acid to evaluate the reported “resistance” of this strain to this neurotoxicant. Utilizing a variety of traditional and specialized histological and biochemical indicators of damage, we observed a temporal manifestation of kainate-induced pathology; extensive damage ensued following limited behavioral seizure activity. Nissl and hematoxylin stains revealed limited neuropathology and identified no overt pyramidal cell loss; however, damaged neurons were revealed in all hippocampal subregions by the more sensitive cupric-silver and Fluoro-Jade B staining methods. Furthermore, neuronal injury was accompanied by both an astrocytic and microglial response. In this “resistant” strain, specialized direct and indirect indicators of damage were required to identify neuropathology, and support the following assertion: standard histological

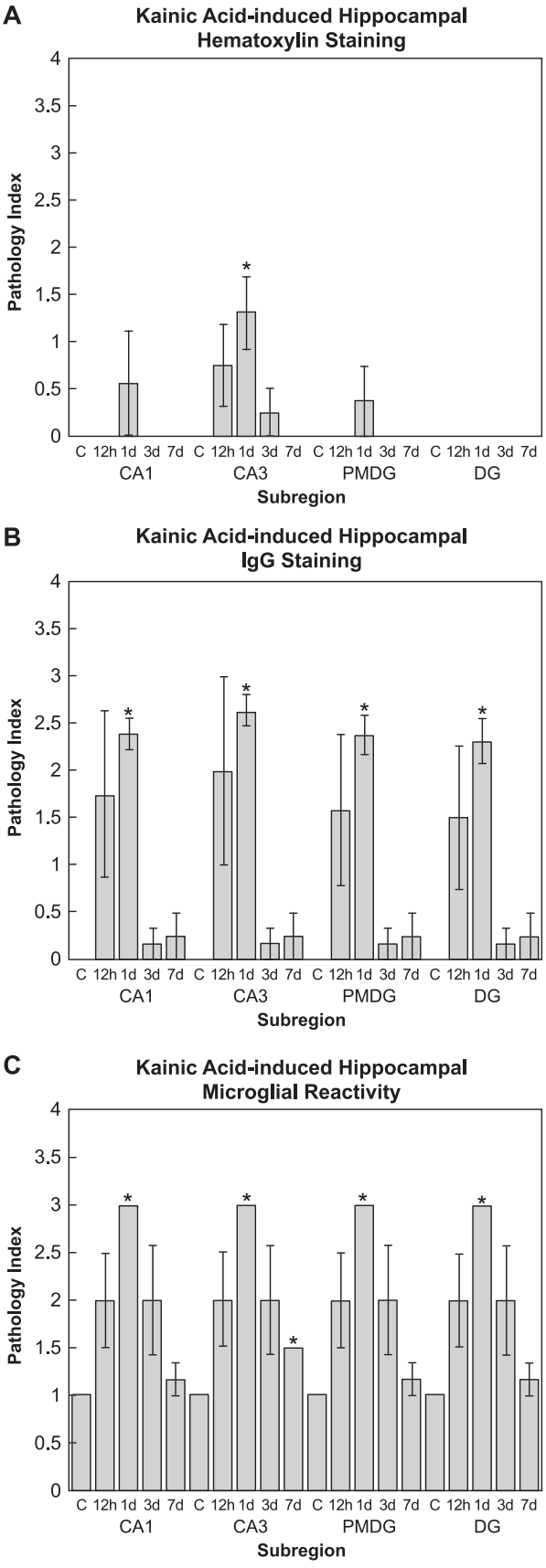

methods may underestimate or fail to reveal existing damage [56,65].

Kainic acid-induced pathology was divided into two categories that were revealed by specific types of histological stains: effects on cellular elements; and effects on the extracellular milieu. The cupric-silver and Fluoro-Jade B stains both revealed treatment-induced damage to neurons and fibers; however, cupric-silver stained sections showed subtle damage to fiber bundles and terminals that we did not observe with FJB. The fixation protocol for the cupric-silver stain requires arsenic-based perfusion and extended incubation in formaldehyde solutions; these procedures may interfere with FJB staining. Terminal damage has been demonstrated in frozen sections of rat brain following treatment with kainic acid [56,57]; however, our use of Permount as a coverslipping media may have resulted in terminal staining being lost in the background fluorescence. Future studies need to determine the relative degree of KA-induced terminal degeneration in the two species. Specific stains that depict the morphology of astrocytes and microglia were performed; these stains revealed morphological alterations consistent with activation of both glial cell types. In addition to cellular effects, kainic acid caused a breach of the blood–brain barrier. Nissl and hematoxylin staining provided important information concerning the identity and topographical localization of non-resident cells that infiltrated the pyramidal cell layer, while immunostaining for IgG revealed extravasation of immunoglobulin into the hippocampal parenchyma.

Genetic influences have been implicated in the differential response of various murine strains to neuropathology following kainic acid treatment [29]; preliminary analysis indicates genetic regulation of seizure activity is complex, and involves as many as eight quantitative trait loci [14]. Further, in reports documenting kainic acid treatment across mouse strains, the correlation between seizure severity and neuropathology is confusing. Seizures are a complex manifestation of underlying aberrant electrical activity in the limbic system; therefore, proof of seizure activity is best determined by direct electrical recording of neuronal activity in treated animals. Due to constraints imposed by the

Fig. 8. Semi-quantitative analysis of histopathology in mice treated with saline or KA. (A) Kainic acid injection caused little significant neuropathology following treatment as revealed by hematoxylin staining. In CA3, a significantly increased number of pyknotic neurons and infiltrating leukocytes was observed at 24 h post-treatment (p=0.028). (B) In CA1, CA3, the polymorphic layer of the dentate gyrus, and the granule cell and molecular layers of the dentate gyrus (DG), significantly elevated influxes of plasma IgG and immunoreactive microglial cells were observed at 24 h post-treatment (p=0.028, 0.028, 0.026 and 0.026, respectively). (C) Kainic acid treatment caused significant elevations in lectin staining and changes in microglial morphology in CA1 and CA3 at 24 h post-treatment (p=0.014 and p=0.014, respectively). In CA3, significantly elevated lectin staining was observed at 7 days post-treatment (p=0.025). In the polymorphic layer of the dentate gyrus, and the granule cell and molecular layers of the dentate gyrus (DG), lectin staining was significantly elevated at 24 h post-treatment (p=0.014 and 0.014, respectively).

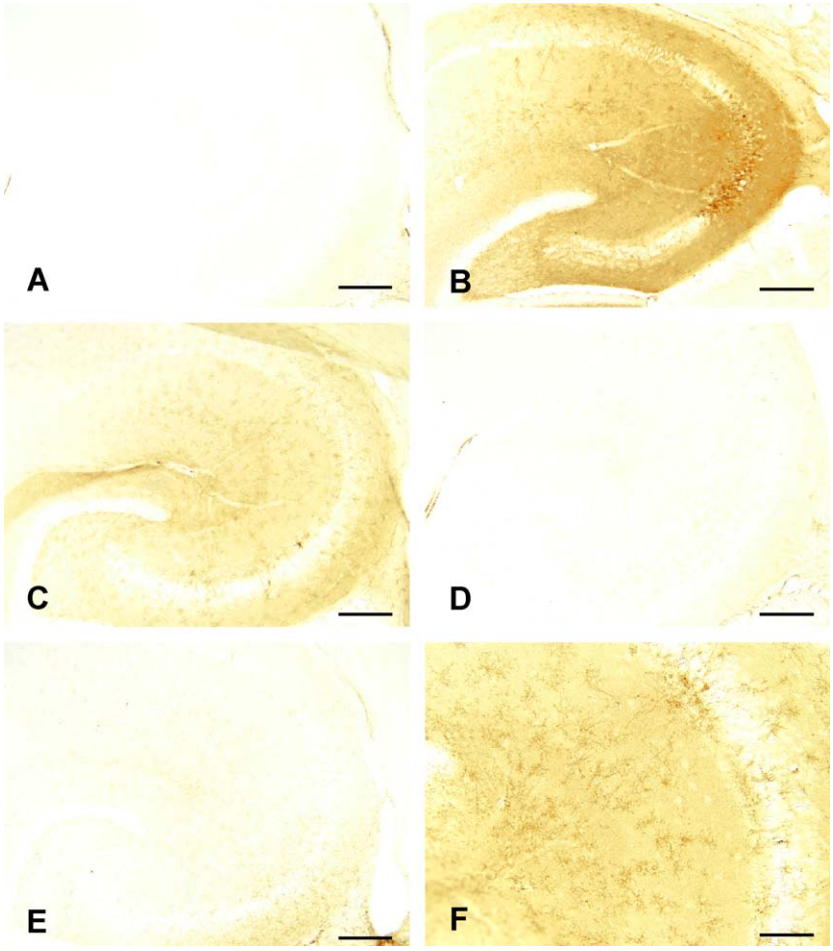

Fig. 9. IgG immunostaining in hippocampus of mice treated with saline or KA. The hippocampus of a saline-injected animal immunostained for IgG showed a lack of immunoreactivity suggesting an intact blood–brain barrier (A). By 12 h following KA treatment, the hippocampal neuropil was immunostained and immunoreactive cells were observed amongst pyramidal neurons (B). By 24 h, profiles of immunoreactive microglial cells were observed throughout the hippocampus (C). By 3 days post-treatment, the quantity of immunoreactive microglial cells was attenuated (D). By 7 days following treatment the hippocampus was indistinguishable from the saline controls (E). Evaluation of immunoreactive cells revealed their identity as microglia (F). Bar in (A–E)=200 μm. Bar in (F)=100 μm.

equipment and expertise required to document neuronal electrical activity, secondary methods have been developed which evaluate seizure severity by observing the behavior of experimental animals [46]. Unfortunately, behavioral seizure scoring is subjective and not standardized between laboratories, and may account for the inconsistent reports of seizure severity following kainate treatment. In our C57BL/6J mice, kainate-induced seizure activity was grouped into two broad categories: animals that seized moderately (stages 1–2 and survived, approximately 75%); and animals that seized severely (stage 5+ followed by death, approximately 25%). Our results are consistent with studies reporting a general convulsion resistance in this strain [13,22,61]. In preliminary experimentation measuring electrical activity in murine hippocampus, we observed treatment-induced electrical patterns indicative of status epilepticus without significant behavioral seizure activity, suggesting central electrical activity may not be reflected in behavior (Dr. Hana Kubova, unpublished observations).

The evaluation of kainate-induced neuropathology is further confounded by the improper selection of histological stains and time courses required to detect damage. All stains utilized in our evaluation of neural damage displayed a graded response that increased to a maximum, then resolved to baseline. The lack of standardized seizure scoring, stains, and time courses used for histopathological analysis has resulted in a confusing literature regarding the relationship between seizure activity and neuronal damage: several studies report higher seizure activity in C57BL/6 mice (stage 3) [17,49], (stages 4–5) [29,55], with no [55], little [29,49] or similar hippocampal neuropathology [17] as reported in our study. In rats, the severity of kainate-induced seizure activity is positively correlated with neuronal damage [54,58]; however, we have shown significant damage in mice in the absence of observable behavior, i.e., tonic–clonic seizures, indicating this correlation is not as strong in the C57BL/6J strain. KA-induced damage in rats was observed as early as 1 h following systemic

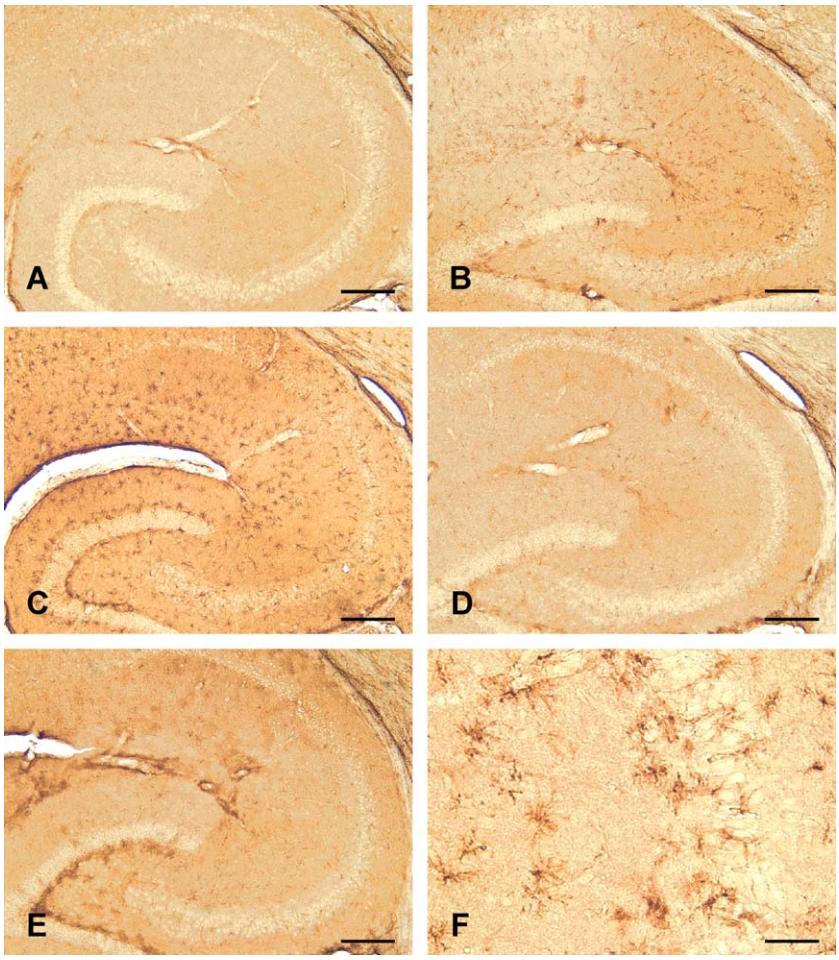

Fig. 10. Lectin staining in hippocampus of mice treated with saline or KA. The hippocampus of a saline-injected animal stained with GIB-4 showed virtually no microglia (A). By 12 h following KA treatment, processes of reactive microglia were observed in CA3 and the hippocampal neuropil (B). By 24 h, entire cells were labeled, and the quantity of stained cells was increased (C). At 3 days, the quantity of lectin-stained cells was attenuated (D). By 7 days following treatment, the hippocampus appeared similar to the saline control (E). High magnification of the pyramidal layer revealed classic activation morphology: a round cell body with few short processes (F). Bar in (A–E)=200 μm. Bar in (F)=50 μm.

treatment [58,60]; the earliest time-point examined in our investigation was 12 h, at which we observed considerable damage. Most indices of KA-induced pathology in our mice resolved by 7 days post-treatment, yet were observed as long as 2 weeks in rats [58,60]; this may either reflect differences in expression of damage signals between rodents, or activation of repair processes following injury.

Previously, we reported GFAP protein levels in C57BL/6J mice were elevated by 24 h following kainate treatment, and were significantly greater than saline-injected controls at 3 and 7 days post-treatment [4]; however, like rats, the high S.E.M. associated with the data reflect individual variability to kainic acid intoxication [15,16,29]. In this series of experiments, we sought to investigate the early time course of KA-induced histopathology, and noted an activation of astrocytes by 12 h. Elevation of GFAP levels provide a reliable indicator of astrocyte activation [11,25], and increase in hippocampus in response to a number of physical and chemical injuries including stab wounds [41], treatment with kainic acid [10], domoic acid [2], and trimethyl tin [5,25,42]. GFAP elevation reflects an increase in the protein content per cell rather than cell division [5], and is characteristic among the morphological changes associated with astrocyte activation.

Whether activated glial cells contribute to excitotoxic neurodegeneration is complex and not completely understood. Activation of both astrocytes and microglia result in the secretion of cytokines and other signaling molecules that may modulate neurotoxicity [62]. Astrocytes responding to kainic acid intoxication release nitric oxide, which may effect neurodegeneration [24,70]. The calcium-binding proteins, S100β [3,18] and calbindin D-28k [26], and the growth factor TGF-β3 [21] are produced in response to kainate treatment and are suggested to promote neuroprotection. Excitotoxin-activated microglial cells produce IL-1β [12,68], tissue plasminogen activator (tPA) [48,59], and nitric oxide [63], which promote neuronal damage, and TNFα [8,34], and TGF-β1 [35] which promote neuroprotection. An examination of these substances following intoxication with kainic acid in C57BL/6J mice may help to

clarify their role in the excitotoxic neurodegenerative process. Whether activated glial cells themselves play a role in the excitotoxic neurodegeneration is less understood; future research focused on the prevention of glial activation following excitotoxicant administration would help determine the role of activated glia in the neurodegenerative process.

The cupric-silver stain revealed considerable neurodegenerative changes in C57BL/6J mice as early as 12 h post-treatment. The major target areas in hippocampus were CA1 and CA3, and to a lesser extent, neurons in the polymorphic layer of the dentate gyrus. We have not observed damage to granule neurons of the dentate gyrus; however, argyrophilic fibers and terminals were found in the polymorphic and molecular layers of severely affected animals. Our data stand in contrast to another study using silver degeneration staining which reports no degenerative changes at doses less than 40 mg/kg at any time-point between 4 and 20 days post-injection [55]. In our experimental paradigm, a dose of 35 mg/kg produced considerable damage at early post-treatment times which was dramatically attenuated by 3 days. Therefore, at the earliest time-point of 4 days [55], the degenerative signal would have resolved to baseline. Numerous studies have shown a relationship between neurodegeneration and argyrophilia; however, the time-dependent nature of the argyrophilic "damage" signal requires an extensive time course, both proximal and distal to treatment, to maximize the detection of neurodegeneration.

Nissl substance consists of polysomes, clusters of ribosomes actively synthesizing proteins; lack of staining by Nissl suggests the biochemical activity of these ribosomes has been attenuated, an effect previously reported to occur following kainate intoxication [6,67]. The transient disappearance of staining suggests that neurons which survived the initial excitotoxic insult may temporarily shut down, yet subsequently recover from hyperexcitation. The non-stained region of the pyramidal layer was not argyrophilic; therefore, neuronal degeneration was presumably not causative of the observed Nissl disappearance. These data suggest kainic acid intoxication in C57BL/6J mice results in an injury that does not progress to overt neuronal loss.

Nissl and hematoxylin staining revealed an infiltration of polymorphonuclear leukocytes into the hippocampus that was most prominent in subregion CA3. Leukocyte infiltration can occur through an intact blood–brain barrier [44]; however, the location of the infiltrating cells corresponded with damage shown by other stains. Further evidence for breach of the blood–brain barrier was provided by immunostaining for IgG, which should be excluded from the brain parenchyma; compared to control animals, kainate-treated mice had significant quantities of IgG dispersed throughout the hippocampal parenchyma. Whether a cause–effect relationship between neuronal damage and blood–brain barrier disruption occurs is not completely understood. BBB damage in mouse brain following kainate intoxication has been reported to be independent of neuronal death [7], and can be attenuated by the anti-malarial drug chloroquine [30], suggesting KA-induced damage to neurons and breach of the BBB occur by different mechanisms. Kainate intoxication has been described to breach the BBB in rats [1,10,23,38,50,66,72] and rabbits [39]. The influx of plasma immunoglobulins and infiltration of leukocytes seen in our mice has also been described in rats [1,47,64]. Whether the entry of leukocytes or other blood-borne factors plays a role in the observed neurodegeneration remains to be determined. Central infusion of autologous plasma, collected prior to kainate treatment, caused no neurotoxicity alone, and failed to exacerbate kainate-induced cell damage [7]; however, whether kainate treatment initiates changes in plasma proteins post-treatment has not been investigated.

Histopathological analysis of brain tissue following neurotoxicant administration has too often been restricted to the use of traditional methods of staining, (i.e., Nissl, hematoxylin and eosin), and evaluation of a single, or few time-point(s) post-treatment. Since many brain regions contain densely packed neurons, significant neuronal loss is required before pathological changes are observed. Our findings suggest that in the evaluation of potentially neurotoxic compounds, sensitive indicators of damage and a comprehensive time-course analysis may be required to reveal underlying neuropathology; our data revealed kainate-induced hippocampal damage in a strain of mouse widely considered to be resistant to excitotoxic neuronal damage. Further, we observed damage in the absence of full tonic–clonic seizures indicating low-level seizure activity may be sufficient to initiate damage and repair mechanisms. The correlation of seizure activity and excitotoxin-mediated neuronal death is important with regard to the use of kainic acid models to investigate mechanisms and develop treatments for human seizure disorders such as temporal lobe epilepsy.

Acknowledgements

The authors would like to thank Brenda Billig for performing the GFAP ELISA, Bridgette G. Balasko for independent scoring of pathology, Dr. Michael Kashon for help with statistical analysis, and Drs. James Antonini and Vic Johnson for internal review of the manuscript. We are also grateful to Dr. Robert Switzer III for excellent technical assistance and valuable discussion.

References

[1] H. Akiyama, I. Tooyama, H. Kondo, K. Ikeda, H. Kimura, E.G. McGeer, P.L. McGeer, Early response of brain resident microglia to kainic acid-induced hippocampal lesions, Brain Res. 635 (1994) 257–268.

[2] N.M. Appel, S.I. Rapoport, J.P. O'Callaghan, J.M. Bell, L.M. Freed, Sequelae of parenteral domoic acid administration in rats: comparison of effects on different metabolic markers in brain, Brain Res. 754 (1997) 55–64.
[3] C. Bendotti, F. Guglielmetti, M. Tortarolo, R. Samanin, W.D. Hirst, Differential expression of S100beta and glial fibrillary acidic protein in the hippocampus after kainic acid-induced lesions and mossy fiber sprouting in adult rat, Exp. Neurol. 161 (2000) 317–329.
[4] S.A. Benkovic, J.P. O'Callaghan, D.B. Miller, Impact of the stress hormone corticosterone on hippocampal response to neurotoxic injury in susceptible and resistant mouse strains, Soc. Neurosci Abstr. 26 (2000) 856.18.
[5] T.O. Brock, J.P. O'Callaghan, Quantitative changes in the synaptic vesicle proteins synapsin I and p38 and the astrocyte-specific protein glial fibrillary acidic protein are associated with chemical-induced injury to the rat central nervous system, J. Neurosci. 4 (1987) 931–942.
[6] A.J. Bruce, S. Sakhi, S.S. Schreiber, M. Baudry, Development of kainic acid and *N*-methyl-D-aspartic acid toxicity in organotypic hippocampal cultures, Exp. Neurol. 132 (1995) 209–219.
[7] Z.L. Chen, J.A. Indyk, T.H. Bugge, K.W. Kombrinck, J.L. Degen, S. Strickland, Neuronal death and blood–brain barrier breakdown after excitotoxic injury are independent processes, J. Neurosci. 19 (1999) 9813–9820.
[8] F. de Bock, J. Dornand, G. Rondouin, Release of TNF alpha in the rat hippocampus following epileptic seizures and excitotoxic neuronal damage, NeuroReport 7 (1996) 1125–1129.
[9] J.S. de Olmos, C.A. Beltramino, S. de Olmos de Lorenzo, Use of an amino-cupric-silver technique for the detection of early and semiacute neuronal degeneration caused by neurotoxicants, hypoxia, and physical trauma, Neurotox. Teratol. 16 (1994) 545–561.
[10] M. Ding, K.G. Haglid, A. Hamberger, Quantitative immunochemistry on neuronal loss, reactive gliosis and BBB damage in cortex/striatum and hippocampus/amygdala after systemic kainic acid administration, Neurochem. Int. 36 (2000) 313–318.
[11] L.G. Eng, R.S. Ghirnikar, Y.L. Lee, Glial fibrillary acidic protein: GFAP—thirty-one years (1969–2000), Neurochem. Res. 25 (2000) 1439–1451.
[12] C. Eriksson, A.M. Van Dam, P.J. Lucassen, J.G. Bol, B. Winblad, M. Schultzberg, Immunohistochemical localization of interleukin-1beta, interleukin-1 receptor antagonist and interleukin-1beta converting enzyme/caspase-1 in the rat brain after peripheral administration of kainic acid, Neuroscience 93 (1999) 915–930.
[13] T.N. Ferraro, G.T. Golden, G.G. Smith, W.H. Berrettini, Differential susceptibility to seizures induced by systemic kainic acid treatment in mature DBA/2J and C57BL/6J mice, Epilepsia 36 (1995) 301–307.
[14] T.N. Ferraro, G.T. Golden, G.G. Smith, N.J. Schork, P. St. Jean, C. Ballas, H. Choi, W.H. Berrettini, Mapping murine loci for seizure response to kainic acid, Mamm. Genome 8 (1997) 200–208.
[15] G.T. Golden, G.G. Smith, T.N. Ferraro, P.F. Reyes, J.K. Kulp, R.G. Fariello, Strain differences in convulsive response to the excitotoxin kainic acid, NeuroReport 2 (1991) 141–144.
[16] K. Hashimoto, K. Watanabe, T. Nishimura, M. Iyo, Y. Shirayama, Y. Minabe, Behavioral changes and expression of heat shock protein hsp-70 mRNA, brain-derived neurotrophic factor mRNA, and cyclooxygenase-2 mRNA in rat brain following seizures induced by systemic administration of kainic acid, Brain Res. 804 (1998) 212–223.
[17] R.Q. Hu, S. Koh, T. Torgerson, A.J. Cole, Neuronal stress and injury in C57/BL mice after systemic kainic acid administration, Brain Res. 810 (1998) 229–240.
[18] K. Huttmann, M. Sadgrove, A. Wallraff, S. Hinterkeuser, F. Kirchhoff, C. Steinhauser, W.P. Gray, Seizures preferentially stimulate proliferation of radial glia-like astrocytes in the adult dentate gyrus: functional and immunocytochemical analysis, Eur. J. Neurosci. 18 (2003) 2769–2778.
[19] E.A. Johnson, D.S. Sharp, D.B. Miller, Restraint as a stressor in mice: against the dopaminergic neurotoxicity of D-MDMA, low body weight mitigates restraint-induced hypothermia and consequent neuroprotection, Brain Res. 875 (2000) 107–118.
[20] C.A. Kassed, A.E. Willing, S. Garbuzova-Davis, P.R. Sanberg, K.R. Pennypacker, Lack of NF-kappaB p50 exacerbates degeneration of hippocampal neurons after chemical exposure and impairs learning, Exp. Neurol. 176 (2002) 277–288.
[21] H.C. Kim, G. Bing, S.J. Kim, W.K. Jhoo, E.J. Shin, M. Bok Wie, K.H. Ko, W.K. Kim, K.C. Flanders, S.G. Choi, J.S. Hong, Kainate treatment alters TGF-beta3 gene expression in the rat hippocampus, Mol. Brain Res. 108 (2002) 60–70.
[22] A.E. Kosobud, J.C. Crabbe, Genetic correlations among inbred strain sensitivities to convulsions induced by 9 convulsant drugs, Brain Res. 526 (1990) 8–16.
[23] H.K. Kulmala, J.W. Boja, J.W. Albrecht, J.T. Hutton, Brain reactive antibodies and the blood–brain barrier: observations in aging rodents and the effects of peripheral kainic acid, Exp. Aging Res. 13 (1987) 67–72.
[24] D.L. Lei, D.L. Yang, H.M. Liu, Local injection of kainic acid causes widespread degeneration of NADPH-d in neurons, endothelial cells and reactive astrocytes, Brain Res. 730 (1996) 199–206.
[25] A.R. Little, J.P. O'Callaghan, The astrocyte response to neural injury: a review and reconsideration of key features, in: D. Lester, W. Slikker, P. Lazarovici (Eds.), Site-Specific Neurotoxicity, Taylor and Francis Publishing, London, 2002, pp. 233–265.
[26] M.P. Mattson, B. Cheng, S.A. Baldwin, V.L. Smith-Swintosky, J. Keller, J.W. Geddes, S.W. Scheff, S. Christakos, Brain injury and tumor necrosis factors induce calbindin D-28k in astrocytes: evidence for a cytoprotective response, J. Neurosci. Res. 42 (1995) 357–370.
[27] M.J. McCann, J.P. O'Callaghan, P.M. Martin, T. Bertram, W.J. Streit, Differential activation of microglia and astrocytes following trimethyl tin-induced neurodegeneration, Neuroscience 72 (1996) 273–281.
[28] B.S. McEwen, E.A. Gould, R.R. Sakai, The vulnerability of the hippocampus to protective and destructive effects of glucocorticoids in relation to stress, Br. J. Psychiatr., Suppl. 15 (1992) 18–23.
[29] G.M. McKhann, H.J. Wenzel, C.A. Robbins, A.A. Sosunov, P.A. Schwartzkroin, Mouse strain differences in kainic acid sensitivity, seizure behavior, mortality, and hippocampal pathology, Neuroscience 122 (2003) 551–561.
[30] J.G. Mielke, M.P. Murphy, J. Maritz, K.M. Bengualid, G.O. Ivy, Chloroquine administration in mice increases beta-amyloid immunoreactivity and attenuates kainate-induced blood–brain barrier dysfunction, Neurosci. Lett. 227 (1997) 169–172.
[31] D.B. Miller, J.P. O'Callaghan, Environment-, drug-, and stress-induced alterations in body temperature affect the neurotoxicity of substituted amphetamines in the C57BL/6J mouse, J. Pharmacol. Exp. Ther. 270 (1994) 752–760.
[32] D.B. Miller, J.P. O'Callaghan, The role of temperature, stress, and other factors in the neurotoxicity of the substituted amphetamines 3,4-methylenedioxy-methamphetamine and fenfluramine, Mol. Neurobiol. 11 (1995) 177–192.
[33] D.B. Miller, J.P. O'Callaghan, Neurotoxicity of D-amphetamine in the C57BL/6J and CD-1 mouse. Interactions with stress and the adrenal system, Ann. N.Y. Acad. Sci. 801 (1996) 148–167.
[34] M. Minami, Y. Kuraishi, M. Satoh, Effects of kainic acid on messenger RNA levels of IL-1 beta, IL-6, TNF alpha and LIF in the rat brain, Biochem. Biophys. Res. Commun. 176 (1991) 593–598.
[35] T.E. Morgan, N.R. Nichols, G.M. Pasinetti, C.E. Finch, TGF-beta 1 mRNA increases in macrophage/microglial cells of the hippocampus in response to deafferentation and kainic acid-induced neurodegeneration, Exp. Neurol. 120 (1993) 291–301.
[36] J.V. Nadler, B.W. Perry, C.W. Cotman, Intraventricular kainic acid preferentially destroys hippocampal pyramidal cells, Nature 271 (1978) 676–677.

[37] J.V. Nadler, B.W. Perry, C. Gentry, C.W. Cotman, Degeneration of hippocampal CA3 pyramidal cells induced by intraventricular kainic acid, J. Comp. Neurol. 192 (1980) 333–359.
[38] C. Nitsch, H. Hubauer, Distant blood–brain barrier opening in subfields of the rat hippocampus after intrastriatal injections of kainic acid but not ibotenic acid, Neurosci. Lett. 64 (1986) 53–58.
[39] C. Nitsch, R. Suzuki, K. Fujiwara, I. Klatzo, Incongruence of regional cerebral blood flow increase and blood–brain barrier opening in rabbits at the onset of seizures induced by bicuculline, methoxypyridoxine, and kainic acid, J. Neurol. Sci. 67 (1985) 67–79.
[40] M.D. Norenberg, Astrocyte responses to CNS injury, J. Neuropath. Exp. Neurol. 53 (1994) 213–220.
[41] J.P. O'Callaghan, D.B. Miller, Neurotoxicity profiles of substituted amphetamines in the C57BL/6J mouse, J. Pharmacol. Exp. Ther. 270 (1994) 741–751.
[42] J.P. O'Callaghan, R.E. Brinton, B.S. McEwen, Glucocorticoids regulate the synthesis of glial fibrillary acidic protein in intact and adrenalectomized rats but do not affect its expression following brain injury, J. Neurochem. 57 (1991) 860–869.
[43] J.W. Olney, T. Fuller, T. De Gubareff, Acute dendrotoxic changes in the hippocampus of kainate treated rats, Brain Res. 176 (1979) 91–100.
[44] V.H. Perry, D.C. Anthony, S.J. Bolton, H.C. Brown, The blood–brain barrier and the inflammatory response, Mol. Med. Today 3 (1997) 335–341.
[45] A. Petzold, D. Baker, G. Pryce, G. Keir, E.J. Thompson, G. Giovannoni, Quantification of neurodegeneration by measurement of brain-specific proteins, J. Neuroimmunol. 138 (2003) 45–48.
[46] R.J. Racine, Modification of seizure activity by electrical stimulation: II. Motor seizure, Electroencephalogr. Clin. Neurophysiol. 32 (1972) 281–294.
[47] R.M. Ransohoff, M. Tani, Do chemokines mediate leukocyte recruitment in post-traumatic CNS inflammation? Trends Neurosci. 21 (1998) 154–159.
[48] A.D. Rogove, S.E. Tsirka, Neurotoxic responses by microglia elicited by excitotoxic injury in the mouse hippocampus, Curr. Biol. 8 (1997) 19–25.
[49] S.J. Royle, F.C. Collins, H.T. Rupniak, J.C. Barnes, R. Anderson, Behavioural analysis and susceptibility to CNS injury of four inbred strains of mice, Brain Res. 816 (1999) 337–349.
[50] R.E. Ruth, Increased cerebrovascular permeability to protein during systemic kainic acid seizures, Epilepsia 25 (1984) 259–268.
[51] R.M. Sapolsky, Glucocorticoid toxicity in the hippocampus. Temporal aspects of synergy with kainic acid, Neuroendocrinol 43 (1986) 440–444.
[52] R.M. Sapolsky, Stress, glucocorticoids, and damage to the nervous system: the current state of confusion, Stress 1 (1996) 1–19.
[53] R.M. Sapolsky, L.C. Krey, B.S. McEwen, Prolonged glucocorticoid exposure reduces hippocampal neuron number: implications for aging, J. Neurosci. 5 (1985) 1222–1227.
[54] R.A. Sater, J.V. Nadler, On the relation between seizures and brain lesions after intracerebroventricular kainic acid, Neurosci. Lett. 84 (1988) 73–78.
[55] P.E. Schauwecker, O. Steward, Genetic determinants of susceptibility to excitotoxic cell death: implications for gene targeting approaches, Proc. Natl. Acad. Sci. 94 (1997) 4103–4108.
[56] L.C. Schmued, K.J. Hopkins, Fluoro-Jade B: a high affinity fluorescent marker for the localization of neuronal degeneration, Brain Res. 874 (2000) 123–130.
[57] L.C. Schmued, K.J. Hopkins, Fluoro-Jade: novel fluorochromes for detecting toxicant-induced neuronal degeneration, Toxicol. Pathol. 28 (2000) 91–99.
[58] J.E. Schwob, T. Fuller, J.L. Price, J.W. Olney, Widespread patterns of neuronal damage following systemic or intracerebral injections of kainic acid: a histological study, Neuroscience 5 (1980) 991–1014.
[59] C.J. Siao, S.R. Fernandez, S.E. Tsirka, Cell type-specific roles for tissue plasminogen activator released by neurons or microglia after excitotoxic injury, J. Neurosci. 23 (2003) 3234–3242.
[60] G. Sperk, H. Lassmann, H. Baran, S.J. Kish, F. Seitelberger, O. Hornykiewicz, Kainic acid induced seizures: neurochemical and histopathological changes, Neuroscience 10 (1983) 1301–1315.
[61] K. Sriram, S.A. Benkovic, D.B. Miller, J.P. O'Callaghan, Obesity exacerbates chemically induced neurodegeneration, Neuroscience 115 (2002) 1335–1346.
[62] K. Sriram, J.M. Matheson, S.A. Benkovic, D.B. Miller, M.I. Luster, J.P. O'Callaghan, Mice deficient in TNF receptors are protected against dopaminergic neurotoxicity: implications for Parkinson's disease, FASEB J. 16 (2002) 1474–1476.
[63] V.C. Stewart, S.J. Heales, Nitric oxide-induced mitochondrial dysfunction: implications for neurodegeneration, Free Radic. Biol. Med. 34 (2003) 287–303.
[64] G. Stoll, S. Jander, M. Schroeter, Inflammation and glial responses in ischemic brain lesions, Prog. Neurobiol. 56 (1998) 149–171.
[65] R.C. Switzer, Application of silver degeneration stains for neurotoxicity testing, Toxicol. Pathol. 28 (2000) 70–83.
[66] L. Sztriha, F. Joo, P. Szerdahelyik, Z. Lelkes, G. Adam, Kainic acid neurotoxicity: characterization of blood–brain barrier damage, Neurosci. Lett. 55 (1985) 233–237.
[67] J.L. Venero, M. Revuelta, A. Machado, J. Cano, Delayed apoptotic pyramidal cell death in CA4 and CA1 hippocampal subfields after a single intraseptal injection of kainate, Neuroscience 94 (1999) 1071–1081.
[68] A. Vezzani, M. Conti, A. De Luigi, T. Ravizza, D. Moneta, F. Marchesi, M.G. De Simoni, Interleukin-1beta immunoreactivity and microglia are enhanced in the rat hippocampus by focal kainate application: functional evidence for enhancement of electrographic seizures, J. Neurosci. 19 (1999) 5054–5065.
[69] O. Vogt, Vogt's method for nerve cell products, in: L.G. Luna (Ed.), Manual of Histologic Staining Methods of the Armed Forces Institute of Pathology, McGraw-Hill, New York, 1968, pp. 212–213.
[70] M.N. Wallace, K. Fredens, Activated astrocytes of the mouse hippocampus contain high levels of NADPH-diaphorase, NeuroReport 3 (1992) 953–956.
[71] S.M. Wuerthele, K.L. Lovell, M.Z. Jones, K.E. Moore, A histological study of kainic acid-induced lesions in the rat brain, Brain Res. 149 (1978) 489–497.
[72] D.K. Zucker, W. G.F., E.W. Lothman, Blood–brain barrier changes with kainic acid-induced seizures, Exp. Neurol. 79 (1983) 422–433.
[73] P.K. Smith, R.I. Krohn, G.T. Hermanson, A.K. Mallia, F.H. Gartner, M.D. Provenzano, E.K. Fujimoto, N.M. Geoke, B.J. Olson, D.C. Klenk, Measurement of protein using bicinchoninic acid, Anal. Biochem. 150 (1985) 76–85.
[74] J.P. O'Callaghan, R.E. Brinton, B.S. McEwen, Glucocorticoids regulate the synthesis of glial fibrillary acidic protein in intact and adrenalectomized rats but do not affect its expression following brain injury, J. Neurochem. 57 (1991) 860–869.
[75] J.P. O'Callaghan, Measurement of glial fibrillary acidic protein, in: L.G. Costa (Ed.), Current protocols in toxicology, 12.81, John Wiley & Sons Publishing, New York, 2002, pp. 1–12.